Carbon Degradation and Kinetics in a Vanadium (4/5) Electrolyte

by
Nicholas Cross

A THESIS

submitted to

Oregon State University

Honors College

in partial fulfillment of
the requirements for the
degree of

Honors Baccalaureate of Science in Chemical Engineering
(Honors Scholar)

Honors Baccalaureate of Arts in International Studies
(Honors Scholar)

Presented May 23, 2017
Commencement June 2017

AN ABSTRACT OF THE THESIS OF

Nicholas Cross for the degree of Honors Baccalaureate of Science in Chemical Engineering and Honors Baccalaureate of Arts in International Studies presented on May 23, 2017.
Title: Carbon Degradation and Kinetics in a Vanadium (4/5) Electrolyte.

Abstract approved:_____

Alexandre F. T. Yokochi

The advancement of the US energy grid is a necessary task to undertake as renewable energies like wind and solar power become more and more prevalent in our energy sector. However, due to uncontrollable factors such as wind speed and cloud cover, the intermittence of these energy sources continues to degrade their viability. In addition, there is a distinct disparity in the time of peak generation and consumption, resulting in an extremely large ramp in output to the grid, which is very difficult for traditional energy sources to produce. In order to compensate for the variability in output of these types of energy systems, large-scale energy storage (LSES) is a viable method for regulating this energy production. Multiple investigations were done into different applications of LSES, such as rural electrification, and the current and future installation of these devices internationally. A main hindrance to the implementation of LSES is the capital costs of installing and maintaining such large batteries. For these reasons, it is essential to understand the longevity and the physical and chemical mechanisms associated with the different potential technologies. A popular LSES option is the redox flow battery which has two main chemistries: iron chloride and vanadium sulfate. This paper investigates the degradation of carbon electrodes and the kinetics in a vanadium (4/5) electrolyte as the cell is cycled thousands of times. Results show that the number of electroactive sites available on the anodic sweep decreases, and that both the oxidation and reduction forward reactions are extremely likely during initial cycling, then the reactions move towards reversible as the cell is continually cycled.

Key Words: vanadium redox flow battery, large scale energy storage, carbon degradation, vanadium reaction kinetics

Corresponding e-mail address: crossn@oregonstate.edu

Carbon Degradation and Kinetics in a Vanadium (4/5) Electrolyte

by
Nicholas Cross

A THESIS

submitted to

Oregon State University

Honors College

in partial fulfillment of
the requirements for the
degree of

Honors Baccalaureate of Science in Chemical Engineering
(Honors Scholar)

Honors Baccalaureate of Arts in International Studies
(Honors Scholar)

Presented May 23, 2017
Commencement June 2017

Honors Baccalaureate of Science in Chemical Engineering and Honors Baccalaureate of Arts in International Studies project of Nicholas Cross presented on May 23, 2017.

APPROVED:

_____

Alexandre F. T. Yokochi, Mentor, representing Chemical, Biological, and Environmental Engineering

_____

Pavel Mardilovich, Committee Member, representing eChemion

_____

Nick AuYeung, Committee Member, representing Chemical, Biological, and Environmental Engineering

_____

Rebekah Lancelin, Committee Member, representing International Degree Program

_____

Toni Doolen, Dean, Oregon State University Honors College

I understand that my project will become part of the permanent collection of Oregon State University, Honors College. My signature below authorizes release of my project to any reader upon request.

_____

Nicholas Cross, Author

Acknowledgements

As independent as a person can be, there is always a multitude of people that are vital to their journey and help guide them at any given point along the path to completion.

Thanks to Dr. AuYeung and Rebekah Lancelin for volunteering time from their busy schedules to be members of my thesis committee. Shout out to Leif Vong for filling in my position for a few months after I left and doing some of the experiments that I did not have time to complete.

Thanks to Dr. Alex Bistrika for having the vision and the entrepreneurial spirit to start eChemion, then allowing me to work in his lab space, despite your feelings towards undergrads using your equipment and not returning it.

Although some of our emails got lost in the ether, if you hadn't responded to a random email from an inexperienced undergrad back in November of 2014, I might not have ever completed a thesis at all. Your perspective on sustainability has shaped mine greatly and your guidance during the writing process was extremely reassuring. Many thanks to my mentor, Dr. Yokochi.

Thanks to all my roommates and close friends that (often unknowingly) were accomplices in my many different procrastination techniques. Thanks to my entire family, my mom, dad, and brother in particular, who have always been supportive of my outlandish work ethic and off the cusp decisions that I seldom consult them about, and who have shaped me into the person that I am today.

The person I probably cannot thank enough for this project would be Dr. Pavel Mardilovich. Somehow you ended up being stuck with me for almost 2 years, but in that time span, you taught me how to be a researcher and how to approach any problem that I have as an engineer. Thanks for all the drawings on the whiteboard, the many conversations about global issues, and all the random stories. You're going to be a great dad.

1. Contents

List of Figures

Figure Page

1. Introduction

1.1. Goal of Thesis

The advancement of the US energy grid is a necessary task to undertake as renewable energies like wind and solar power become more and more prevalent in our energy sector. However, due to uncontrollable factors such as wind speed and cloud cover, the variability of these energy sources continues to degrade their viability. In addition, there is a distinct disparity in the time of peak generation and consumption, resulting in an extremely large ramp in output to the grid, which is very difficult for traditional energy sources to produce. In order to compensate for the variability in output of these types of energy systems, large-scale energy storage (LSES) is a viable method for regulating this energy production. A main hindrance to the implementation of LSES is the capital costs of installing and maintaining LSES technologies. For these reasons, it is essential to understand the longevity and the physical and chemical mechanisms associated with the different potential technologies.

1.2. Thesis Statement

One prominent LSES technology is the vanadium redox flow battery, which has complex kinetics and degradation mechanisms. The goal of this thesis is to investigate the rate of degradation of carbon electrodes and the kinetics of the 4/5 reduction-oxidation couple of vanadium in an electrolytic solution.

2. Background Information

2.1. Necessity of Large Scale Energy Storage (LSES)

As the percentage of US citizens that are in favor of alternative energies continues to rise, so does the necessity to accommodate for the intermittency of renewables in our electrical grid.[1] Due to their nature, sources such as wind and solar cannot be fully relied upon as a complete source. Rather, a baseload such as nuclear or coal is still necessary, but renewables are often used during peak power so a significant ramp is not required from the baseload source. A significant problem with solar and wind being intermittent is that they are not predictable, resulting in our inability to plan around the changes in power that are produced by those sources. While the prediction of these sources is a key part in increasing the prevalence of renewables, the discussions in this thesis will focus on the ways to use LSES as a means to mitigate the fluctuations from these sources. Energy storage technologies are being installed more commonly as a method to complement renewable sources because of their ability to provide the grid with exactly the amount of energy that it needs. Since the range of response time needed from the storage system can vary from seconds to hours or days, the right type of storage system needs to be chosen and designed for the energy market in which it will be a part of.

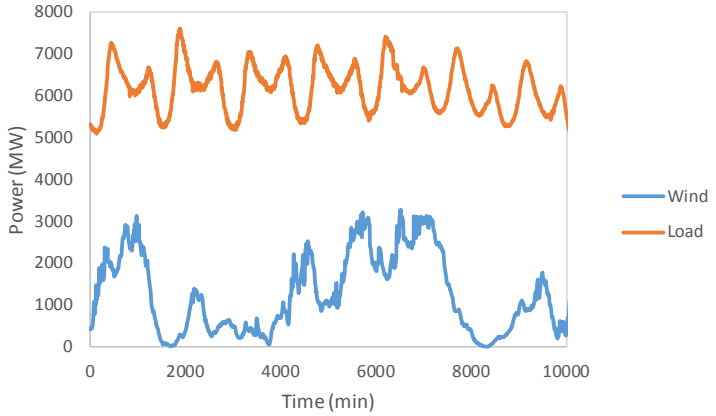

a)

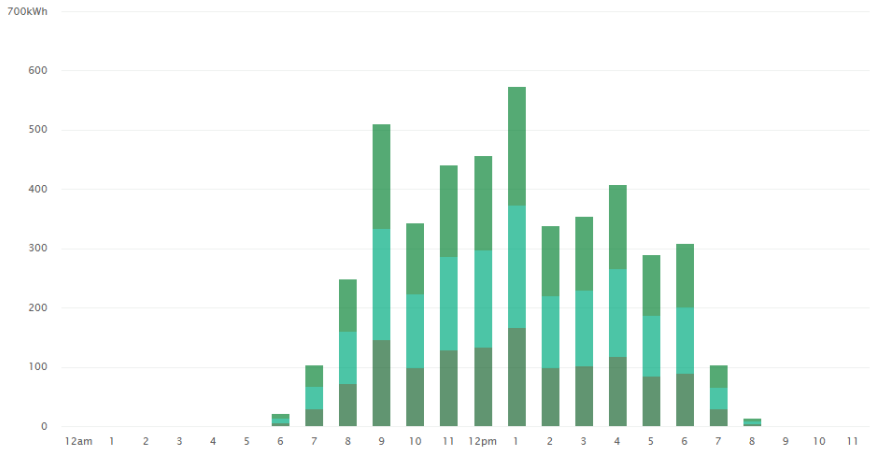

b)

Figure 1: Real-time data demonstrating the intermittence of different renewable sources, a) wind power produced over six days relative to the system load (courtesy of Bonneville Power Administration)[2], and b) the variation of solar power in one day because of cloud cover (courtesy of SolarCity)[3]

The data represented in Figure 1 demonstrates how both a) wind and b) solar energy can fluctuate greatly in relatively short periods of time, perfectly showing their need for a complementary energy storage system. One example is that there is a period of roughly 1000 minutes (16.6 hours) where there is little to no wind energy being produced. Another is a fluctuation of 45% (about 250 kWh) is seen in the span of one hour in the power produced by the solar farm. These two examples show the need for types of energy storage with different response times to accommodate for the rate of fluctuation in the energy being produced. There is also a large push for the installation of renewable energies internationally, with some studies showing that developing countries are investing more into them than developed countries.[4]

2.2. Effect of the "Duck Curve"

With increasing penetration of solar energy and with the progression of the daily load distribution, the necessity for energy storage technologies becomes clear because of the possibility of overgeneration. The risk of overgeneration is becoming more and more prevalent as residential energy usage becomes more efficient, causing to the load to drop during the middle of the day, and this phenomenon is known as the "duck curve" because of the resemblance of the shape of the curve. Potential results from this include an increase in the cost of the energy

production and the increase in CO_2 emissions, which is the antithesis of the objective of renewable resources.[5]

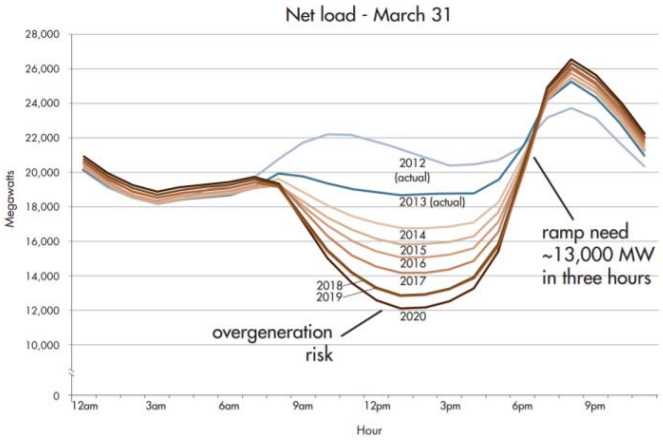

Figure 2: Sample duck curve showing the potential for overgeneration due to the penetration of solar energy technologies. Courtesy of the California Independent System Operator[5]

As the load during the middle of the day begins to sink, the need for storage increases to prevent overgeneration, as shown in Figure 2. An explanation of this phenomenon is that the power produced by renewables tends to decrease after the sun peaks for the day, as well as total usage on the grid increases as people return to their homes after work. This requires a large ramp in production from the sources of either baseload or peaking power. This large ramp in production poses a significant problem for the current energy grid because baseload power sources such as nuclear and coal are not able to ramp their production at the rate that would be necessary. Sources for peak power are often natural gas turbines which produce a significant amount of carbon emissions. This means that even places that use non-carbon sources for their baseload power can still end up using carbon fuel sources in order to accommodate for peak power. Additionally, solar and wind energy are too intermittent to be considered reliable sources for providing the ramp in power. On the other hand, many forms of LSES are able to discharge their power at this rate and store enough energy to compensate for the change in load, making them a common idea for a solution to this pressing issue.

2.3. Usage in Rural Electrification

With the progression of a society comes the increased need for services such as easily accessible potable water, civil infrastructure, and electricity. Currently, many countries in African and Southeast Asia use oil and coal as their method for providing power, much of which must be imported at prices that are out of their control and can be too expensive for the population to afford.[6] As the economies of these countries grow, and their populations increase, this will result in an exponential increase in carbon emissions that could be avoided by altering how these areas produce power. By providing the resources for sustainable energy production early, this will allow them to skip over the phase in their development where the large, industrialized population relies on cheap, dirty power, and instead will expand their already existing renewable energy infrastructure.

Traditionally, electricity is generated at a plant just outside the central population hub, then carried into and distributed around the municipality. This strategy works well in moderately developed, urban areas, however a different approach is needed in order to supply electricity to rural towns in places such as Africa and Southeast Asia. While power still must be generated in a central source, the capital cost of distribution is too high and the energy usage is too low to for a carbon-based power plant to be considered cost effective, especially considering that the fuel must constantly be shipped into an area with little infrastructure.[7] These factors make rural villages great candidates for being supplied completely by renewable energy sources. This will be especially beneficial for mitigating future carbon emissions, as these areas are likely to see a decline in infant mortality rates soon that will result in a large population increase. This population increase is directly correlated to the carbon emissions of these areas, as they will rely upon cheap sources of fuel such as coal and natural gas.

Of the 1.3 billion people that do not have access to electricity, a staggering 95% of them live in either sub-Saharan Africa or developing Asia, and 84% of them live in rural areas.[6] A distribution of the specific countries that these people live in is located below in Table 1.

***Table 1**: Breakdown of countries that have specifically high populations of citizens without access to electricity (data from 2009)[6]*

Without access to electricity	**Population (million)**	**Share of Population**
Africa	587	58%
Nigeria	76	49%
Ethiopia	69	83%
DR of Congo	59	89%
Tanzania	38	86%
Kenya	33	84%
Other sub-Saharan Africa	310	68%
North Africa	2	1%
Developing Asia	675	19%
India	289	25%
Bangladesh	96	59%
Indonesia	82	36%
Pakistan	64	38%
Myanmar	44	87%
Rest of developing Asia	102	6%
Latin America	31	7%
Middle East	21	11%
Developing Countries	1314	25%
World	1317	19%

This data offers targets for those looking to aid the countries least equipped to solve the problem of providing electricity for their citizens on their own. However, many of these countries have problems with internal wars and corrupt politicians that often dissuade anyone from aiding them because of their fears that their investment will go to waste. This issue sheds light on the human element of engineering that is the implementation of technologies is heavily dependent upon the politics of the area that where the technology is to be used.

In planning the creation of a rural electrification system, many decisions go into the preparation of the system and determining the most effective energy source and energy storage

technology. These will vary from location to location based on factors such as the climate, the geography of the area, and the necessary energy requirements for the village. The most common types of renewable energy sources for this application are hydro, wind, and solar power, and an energy storage system is often necessary to accompany these sources.[8]

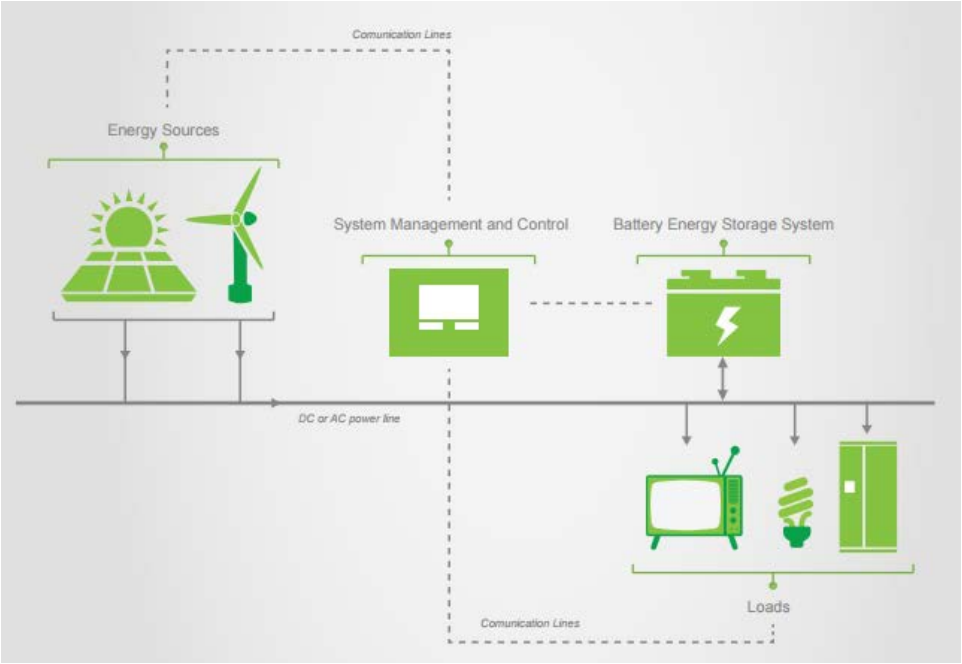

Figure 3: Diagram of a basic rural electrification system[7]

Renewables, especially wind and solar, usually are low maintenance and have low operating costs, both are which are very positive for usage in rural areas. However, they both have high capital costs, and if a part does malfunction, it would likely be very difficult for the local community to find a proper replacement relatively close to their village.[8]

The energy storage systems used in the electrification system play a central role because of the fluctuation of renewables and potential for overgeneration, meaning that the energy storage system can be thought of as the baseload power source for the village. The storage time for these systems is often not longer than hours, and therefore electrochemical batteries are the favored storage system.[7] The quick response that is often needed to accommodate for rapid

changes in the amount of energy produced by solar or wind power can easily be handled by a battery system without resulting in large surges on the grid. In addition, because of the nature of batteries, their storage capabilities are able to simply be stacked as the village grows and begins to produce more power, and therefore requiring more storage.

2.3.1. Residential Energy Storage Systems

Another example of an application for energy storage is within a microgrid, where the power production and control is delocalized from a large, central power station to allow for more efficient production based on the power usage of that geographical area.

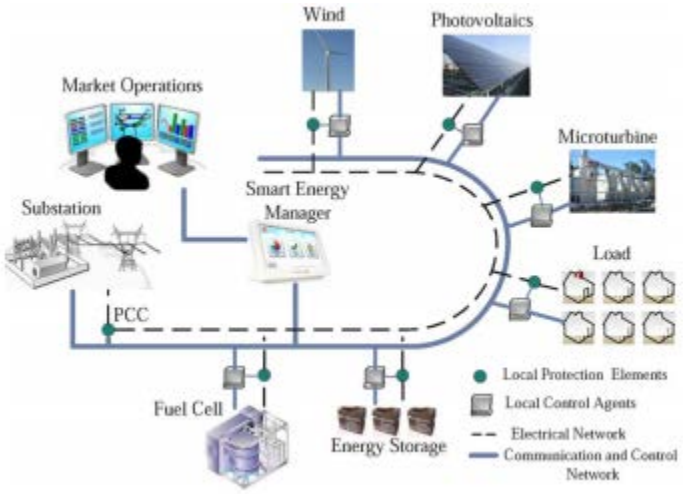

Figure 4: An example of a microgrid[9]

A microgrid can be considered analogous to a system set up for rural electrification because the load is so close in proximity to the power sources. Energy storage is required for microgrids because of the potential for the frequency and voltage to fluctuate based off supply received from renewables and the demand from the buildings on the grid.[10] An example for a grid is simply a large neighborhood, so large fluctuations could be from sources such as turning on and off large appliances, charging of electric vehicles, or people leaving for or coming home from work. In order to properly balance the load on the system, an energy storage system is required for both small

fluctuations in the load, or large fluctuations from the power received from a renewable power source.[10]

2.4. Types of LSES

2.4.1. Pumped Hydro and Compressed Air Storage

Pumped-storage hydro power is the most common form of energy storage in the world, as most of the technology used has been around for many decades.[11] The basic concept of a pumped hydro system is that there is a reservoir of water held at high elevation, and when power is needed, the water flows downhill to a lake, spinning a turbine and creating electrical energy. To "refuel" the system, the water in the lake can then be pumped back up the hill to the reservoir. This pumping of the water back up to the reservoir often happens during non-peak hours as this makes it so the baseload power sources do not have to ramp their production and because the electricity can be bought at a much cheaper price.[11]

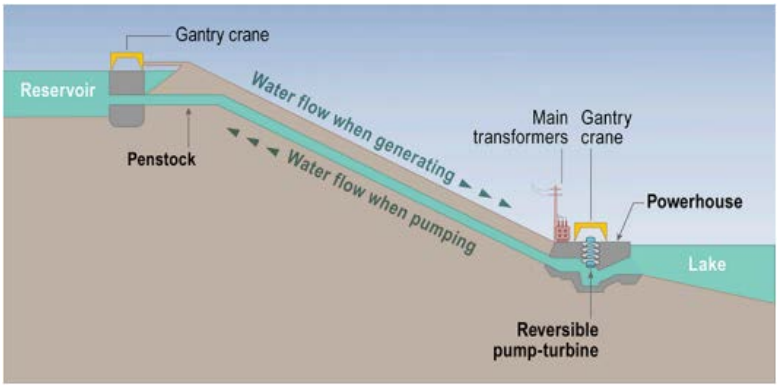

Figure 5: Sample representation of a pumped hydro facility[11]

Pumped hydro is most commonly installed in very large (gigawatt scale) sizes because it is most commonly used for longer-duration applications such as load leveling.[12] It is also a good complement to baseload power because it can ramp up and down quickly to accommodate for peak load requirements.[11] One of the main drawbacks of pumped hydro are the geographic requirements for the systems because there needs to be multiple water sources close together

that also have a change in elevation. There are also potential environmental concerns because the disruption of the flow of a river or taking water in and out of a lake could significantly impact the wildlife in those habitats.

Compressed air energy storage (CAES) is a very similar process to pumped hydro, with the two key differences being that air is used in place of water, and the air is stored in an underground cavern. CAES can be ramped faster than pumped hydro, but is much less common because of its reliance on geological formations for containment of the air, especially considering the large volume required to contain enough air to produce a viably sized energy storage plant.[11] CAES is considered to be a hybrid generation process because it requires the combustion (most often natural gas) to produce power, and therefore still producing carbon emissions. The higher pressure of the system does allow for a slightly higher efficiency within the gas turbine.

2.4.2. Flywheels

A flywheel is a mechanical device that stores energy as rotational kinetic energy of a rotating mass. An electric energy input is transferred into and out of a flywheel by an electric motor, which in turn leads to high efficiencies, upwards of 95%, compared to that of 60 to 80% for other energy storage technologies.[13] The energy is stored through the use of inertia and the rotational movement of the mechanical parts within the flywheel. Due to the nature of their design, flywheels offer good response for shorter fluctuations in the load on the grid, but they are not able to store a significant amount of energy.[12]

2.4.3. Molten Salt/Thermal Systems

Molten salt, or thermal, energy storage systems store energy as sensible heat which can be transferred to a steam turbine to produce power. Because the energy is being stored in a

molten-solid state, the operational temperature of these storage systems is often well above 350 °C, which could become a safety hazard in the event of a malfunction.[14] These systems are often used for peak power applications because they are best suited for durations on the magnitude of multiple hours.[12] A common use for molten salt storage is in a solar concentrator farm, where the solar tower can get up to multiple thousands of degrees Celsius, therefore being well suited for an energy storage system that can operate at a similar temperature.

2.4.4. Electrochemical Batteries

Often batteries are broken down into two main categories: wet cell, and redox flow batteries. Wet cell batteries are extremely more common with examples including lithium-ion, nickel metal-hydride, and lead-acid, while flow batteries are a more developing technology where the main species used are vanadium sulfate, zinc bromide, or iron-iron chloride. Both types can be useful for both long and short durations and are useful for both small and large amounts of energy.[12]

For LSES applications, lithium-ion batteries are currently the most common wet cell technology used because they are easy to stack, and they have high power and energy ratings, relative to the mass of the battery. They are often used for peak power with durations being on the order of hours, and are often a primary choice for rural electrification systems because of their relatively low capital costs.[7] There has been much research into the development of lithium-ion batteries over the last few decades because of their wide variety of applications, with major developments resulting in both higher energy density and increased power of the cell. There has been significant research done in developing batteries using different alkali metals, but most other metals are considered to be poorer because of their lower reduction potential or scarcity.[12]

The technology for redox flow batteries (RFBs) has been around for some time (since the 1960s), but they have not gotten much significant attention until quite recently. Currently, they are being investigated for LSES applications with higher energy requirements somewhat exclusively, as their design does not allow them to be very competitive in small scale applications.[12] RFBs use chemistry that is very similar to that of wet cell batteries, except they separate the different components into distinct sections of the battery. The electrochemically active species, the anolyte and catholyte, are stored in liquid form in tanks outside of where the redox reactions take place, and pumped into the reaction area. A generic setup for an RFB is shown in Figure 6. One specific popular chemistry is the vanadium redox flow battery (VRFB) which uses an anolyte that is a mixture of vanadium (II) and (III), and a catholyte that is a mixture of vanadium (IV) and (V), with an electrode that is often some form of graphitic carbon.

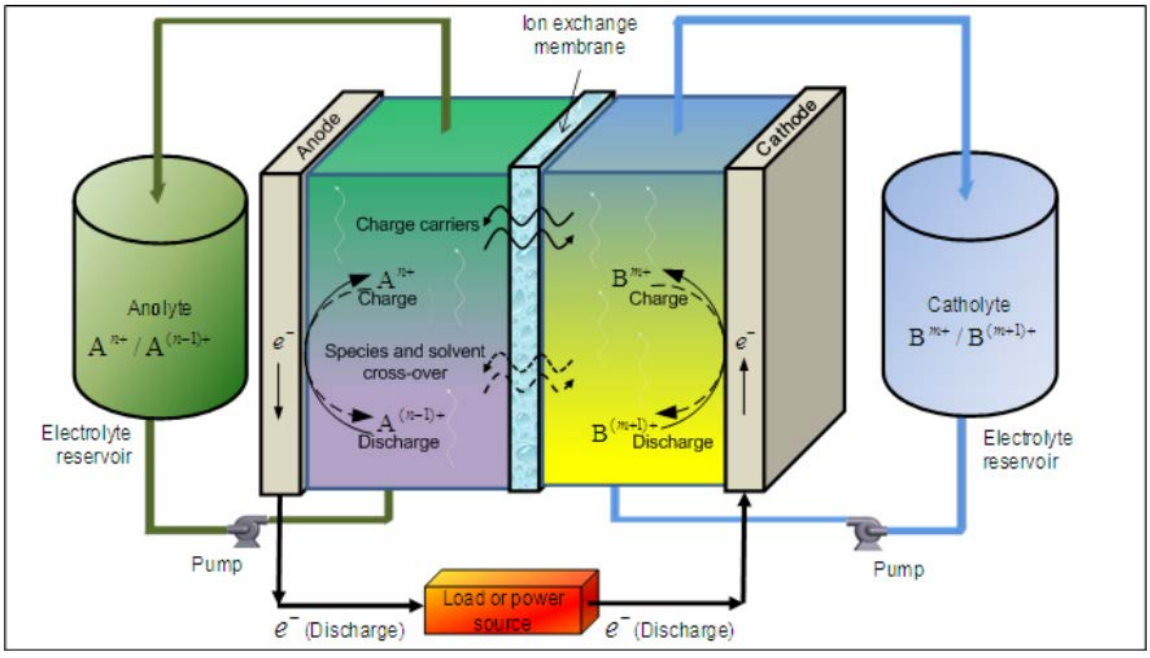

Figure 6: Generic design and basic chemistry of an RFB[12]

One primary advantage of the RFB design is the separation of the total energy stored and the potential power output of the battery. The amount of energy is only dependent upon the volume of the anolyte and catholyte tanks, while the power is dependent upon the size of reactor

stack.[12,15] This characteristic allows for great variability and customization in the design of the RFB and allows for them to be used in a wide variety of applications within the energy storage market, which is why many consider them to be a promising technology for the future of grid technology. Additional benefits include the safety of design of RFBs, as aqueous chemistry is inherently inflammable (although some RFB chemistries use corrosive acids, such as sulfuric acid in vanadium RFBs), and the relative abundance of metals such as iron and vanadium in the earth's crust is comparable to or higher than that of lithium.

2.5. International Usage of Energy Storage

Internationally, energy storage techniques are used on a large scale, with there being a total of over 100 GW of power currently installed around the world, including all types of technologies. The data analyzed in this section is courtesy of the DOE Global Energy Storage Database. There are four types of energy storage considered for this analysis: pumped-hydro, electrochemical, electromechanical (primarily flywheels), and thermal storage. While many more technologies exist, these categories were chosen because they are by far the most prevalent in the energy storage market.

Energy storage types and applications are quite diverse internationally, but pumped hydro storage dominates the current landscape because the technology is simple, and has been used on a large scale since early in the 20th century. Part of the reason that it has such a significant representation of the amount power produced is because the installations are almost always on the scale of 100s to 1000s of megawatts of power. It was chosen to sort the data by power because it better represents the scale of the systems that are built, as well as the priority of the type of storage facility installed. The data could be sorted by the number of installations, but that would skew the data to show a large number of electrochemical and thermal storage systems.

This is because there are a large number of these systems, but they do not have large storage capabilities, with some being as low as 1 kW for use in a microgrid case study.

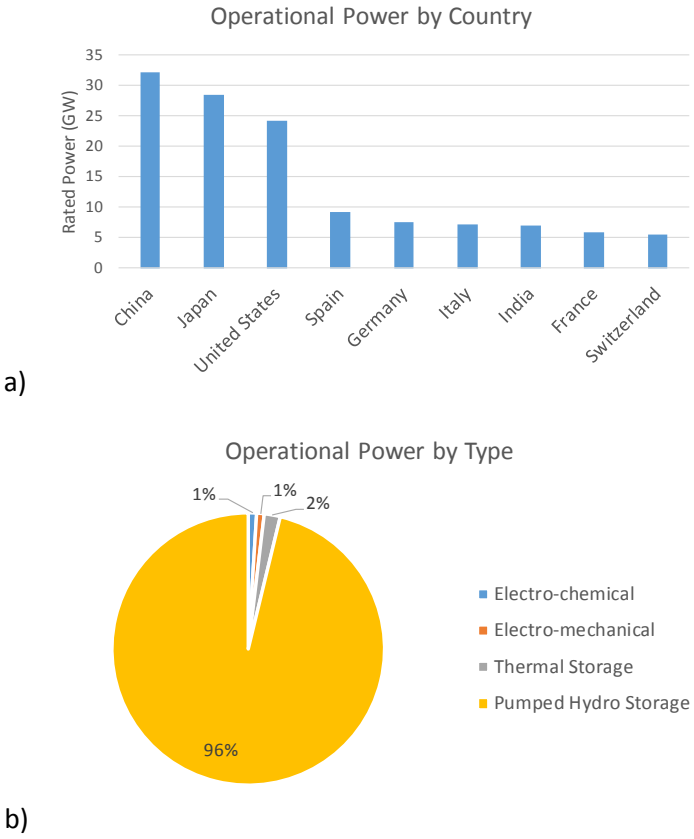

Figure 7: a) Highest 9 countries for current operational power of energy storage b) Distribution by type of energy storage of current operational power for all countries

As shown in Figure 7a, China, Japan, and the United States lead the world by far with their current amounts of energy storage installed and operating. China and the United States both have had a significant amount of pumped hydro storage because of the large areas of land that these countries occupy, and therefore number of rivers and lakes that they have access to for construction of these installations is significantly higher than other countries. In addition, China and the US are by far the two largest energy consumers in the world, and having pumped hydro installations can help decrease their dependency upon importing foreign energy. Japan is not nearly as large of a country, but their topographical layout favors pumped hydro very well, and

they have had the economy and support from their populace to install a large amount of renewable energy sources. No individual country in the European Union has nearly the capacity of any of these countries, likely due to their smaller sizes, but if the EU as a whole is considered, then they would be at the top of the list for total power.

Looking at the future, the United States and Canada represent a large portion of the power that has been announced to be installed. This exemplifies a difference in focus between North America and the rest of the world on how they are going to renewably provide energy for their populations. Due to recent events, such as the Fukushima disaster in Japan and Germany voting to decommission all of their nuclear power plants, there is more of a focus on the installation of safe and renewable energy production technologies, as opposed to energy storage. While this will likely lead to the increase in LSES installations in the future, LSES is not the focus in their current projects. However, with the recent change in the US administration and proposed budget cuts to the US Department of Energy and the Environmental Protection Agency, the amount of energy storage that the US will install could decrease drastically.

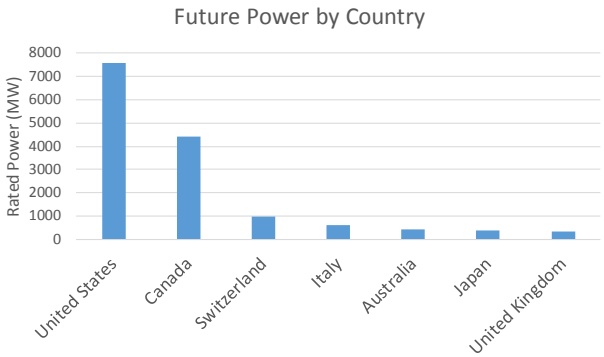

a)

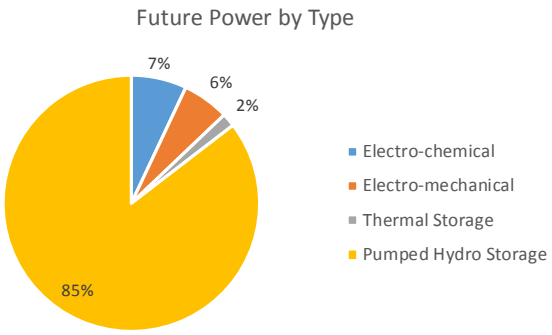

b)

Figure 8: a) Highest 7 countries for announced or under construction energy storage, based off rated power b) Distribution by type of energy storage of announced or under construction installations for all countries

Figure 8b shows a change in focus in the types of technology being installed in energy grids around the world. This distribution of energy types is consistent between the US and Canada, with them both having a few large powered pumped hydro installations planned, and several smaller installations of batteries and flywheels. The distribution is not as consistent within other countries because of the smaller number of installations that they currently have planned. The growth in the amount of electrochemical and electromechanical reveals the growth in renewable sources and the investigation into the installation of microgrids. This information bodes well for mitigating carbon emissions worldwide and showing an international effort in decreasing the amount of fossil fuels used for power production.

2.6. Electrochemical Theory

Electrochemistry is the study of reduction-oxidation reactions which occur when one reactive species loses an electron (oxidation), and that electron is transferred to and gained by another reactive species (reduction). If the system is setup such that the electron transfer happens through a spontaneous reaction, this is referred as a galvanic cell, but if the reaction is forced by a potential put across the two reactive species, it is a electrolytic cell.[16] This thesis

analyzes an electrolytic cell where the reacting species are different oxidation states of vanadium, using a three-electrode setup consisting of a working, counter, and reference electrode.

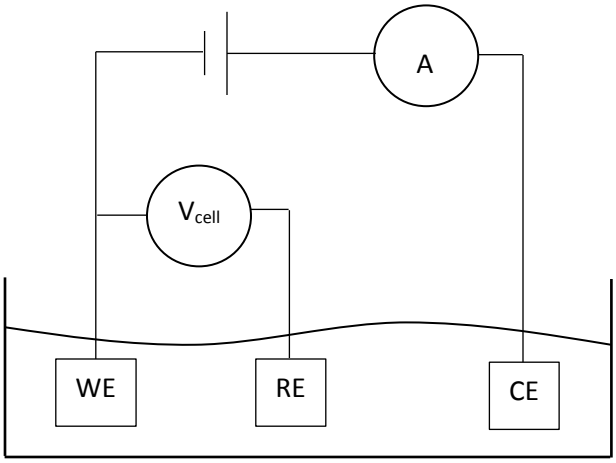

Figure 9: Drawing of a three-electrode setup

The working electrode is where the reaction is taking place, and therefore the electrode of focus for any analysis done on the system. The surface area exposed to the electrolyte must be kept constant, as to set a current density across the entire electrode.[16] The counter electrode is used to balance the current produced at the working electrode. This material does not participate in the reaction, and thus needs to be made of an inert material and have a larger surface area to ensure that it is not the limiting factor in the kinetics of the reaction.[17] The reference electrode has a known reduction potential, and acts as a mechanism to determine the voltage of the working relative to the reference electrode. Ideally, there is no current passing through the reference electrode, and this allows the electrochemical reaction at the working electrode to be fully characterized.[16]

One major governing equations within electrochemistry is the Nernst equation, shown below. The Nernst equation dictates the thermodynamics of an electrochemical system and is used for relating the potential of an electrochemical cell to the electrolyte used during experimentation, and the activities of the oxidizing and reducing species.[16]

$$E_{cell} = E^{o}{}_{cell} - \frac{RT}{zF}\ln\frac{a_{Red}}{a_{Ox}} \quad (1)$$

The Tafel equation governs the kinetics of an electrochemical system, and is shown in Equation 2. The Tafel equation relates the overpotential (η) of the cell to the current resulting from the cell by two key parameters, the charge transfer coefficient (α), and the exchange current density (i_o), as a function of the reaction rate (i) in C / s.

$$\eta = \frac{kT}{e\alpha} * \ln\frac{i}{i_o} \quad (2)$$

The charge transfer coefficient is often thought of as the readiness of the system to react or the likelihood for the forward reaction to occur. The exchange current density is correlated to the number of active sites for either the oxidation or reduction reaction to take place within the electrode. The Tafel equation is a simplified version of the Butler-Volmer equation where the sweep is done to high overpotentials.[17]

2.7. Electrochemical Testing Methods

2.7.1. Cyclic Voltammetry

For a reversible electrochemical reaction, cyclic voltammetry is a method that can be used for analyzing reaction mechanics and the reactive species in the electrolyte.[16] The technique sweeps the voltage linearly from below the oxidation peak to above the reduction peak and back to charge and discharge the working electrode. The resultant current is dependent upon the active surface area of the electrode and the ability of the active species to diffuse to the working electrode.[16] Typically, and as was done in this research, the electrolyte is not stirred in order to observe the effects of mass transfer on the system; this is in contrast to a Tafel Test where the electrolyte is not stirred because the governing equation does not take into account the effects of mass transfer. Figure 10 shows a sample cyclic voltammogram, detailing which peak corresponds to either the cathodic or anodic side of the reaction.

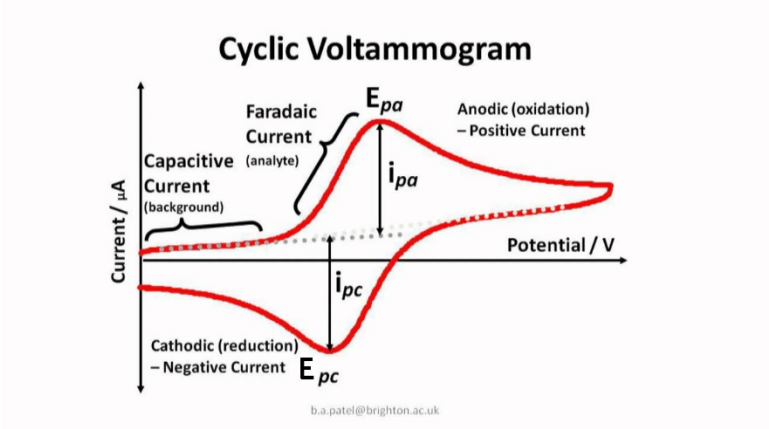

Figure 10: Sample cyclic voltammogram[18]

Potential is plotted on the horizontal axis to show the forward and reverse reactions happening in the same cell, but with reversed polarity.[16] Repeating this test many times sweeping to a high overpotential simulates cycling of a battery, causing the carbon electrode to degrade.

2.7.2. Tafel Test

In analyzing the kinetics of an electrochemical system, a Tafel plot is a common technique that plots the relationship between the overpotential and the current on a logarithmic scale. This test can be somewhat sensitive, as it is usually only valid within a few hundred millivolts of overpotential around the open circuit potential (the voltage applied to the cell that results in no current).[17] Figure 11 shows a sample Tafel plot, and the equations associated with the analysis of this plot. The parameters for the equations are: α, the transfer coefficient; F, Faraday's constant; R, the gas constant; and T, the temperature of the cell.

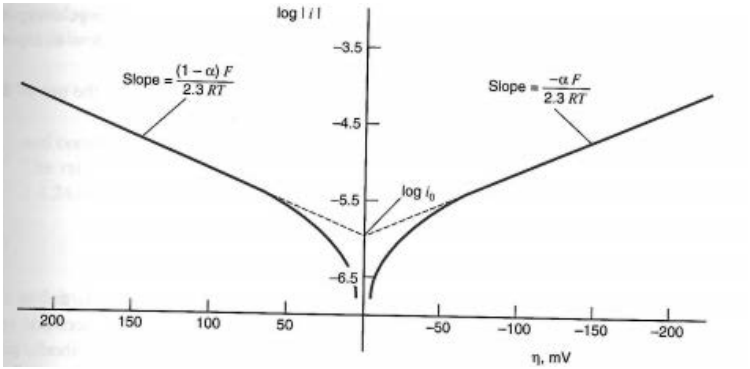

Figure 11: Sample Tafel plot where the line on the left is the anodic current and the line on the right is the cathodic current[17]

3. Experimental Methods and Materials

3.1. Electrolyte Preparation

The electrolyte used was a mixture of 0.25 M V(III) with 0.75 M V(V), in a 3 M H_2SO_4 solution. The V(III) in the solution came from a V_2O_3 oxide purchased from Alfa Aesar, and the V(V) in the solution came from a V_2O_5 oxide purchased from Aldrich. Creation of the solution began with 68.21 g of V_2O_5 and 187 mL of H_2SO_4, diluted to about 900 mL. After this, the 18.74 g of V_2O_3 was added, then deionized water was added until the solution was 1 L, left heated and stirring for two weeks. This resulted in a solution with 1M vanadium with an average oxidation state of 4.5, corresponding to a 50% state of charge of a positive electrolyte.

3.2. Electrode Preparation

A three-electrode setup (working, counter, and reference) was used during the experimentation. The counter electrode used was simply a graphite rod with one tip being flattened into a rectangular shape to ensure a consistent contact with the leads from the potentiostat. A $Cu/CuSO_4$ reference electrode was used in all experiments, and the copper wire was encapsulated by two separate containment systems for saturated copper sulfate. The inner containment system was a thin glass tube, sealed on each end, and the porous membrane being a glass frit. The outer containment system was a thin glass pipette with the tip filled with cloth. This electrolyte is light-sensitive, so during testing an opaque jacket was used to shield the electrode from being affected by light and keep the measurements consistent.

The working electrodes used were wax-impregnated graphite rods, 0.5” long and 0.25” in diameter. The impregnation was completed by melting paraffin wax and submerging the electrodes in the melted wax, and was done to minimize the porosity of the electrodes. After the electrodes were removed and cooled, wires were connected using silver epoxy and the all sides but the active surface were coated with paraffin wax to keep the area interacting with the

electrolyte a constant size and orientation. The surface of the electrode was prepared in such a way to ensure the face is consistently flat and that the peak spread on a cyclic voltammogram is minimized. The electrode was put through a series of polishing steps, 320 and 600-grit sand paper followed by 5 micron alumina polish, to produce a smooth polish. In between each step, the electrode was sonicated in a 0.1 M solution of sodium dodecyl sulfate to remove all the loose particles from the surface of the electrode. Last, the electrode was submerged in 10% by volume nitric acid for 10 minutes as way to activate the surface.

In the three-electrode setup, it is standard practice for the surface area of the counter electrode to be much larger than the working electrode, to ensure that the counter electrode is not the limiting area for the reaction to occur. The following calculations show the difference in the area between the counter and the working, given that both of their radii are 0.318 cm and the counter is submerged about 1.91 cm.

$$SA_{WE} = \pi {r_{WE}}^2$$

$$SA_{WE} = \pi (0.318)^2$$

$$SA_{WE} = 0.316\ cm^2$$

The surface area of the working electrode is 0.316 cm^2.

$$SA_{CE} = \pi {r_{CE}}^2 + 2\pi r_{CE} h_{CE}$$

$$SA_{CE} = \pi (0.318)^2 + 2\pi (0.318)(1.91)$$

$$SA_{CE} = 4.12\ cm^2$$

The surface area of the counter electrode is 4.12 cm^2, and therefore 13 times greater than the working electrode.

3.3. Instrumentation and Test Parameters

A 20 mL vial was used to contain the electrolyte and electrodes, and the tests used a Gamry Instruments Reference 3000 potentiostat. Figure 12 shows the setup of the system on the stir plate, not including the potentiostat.

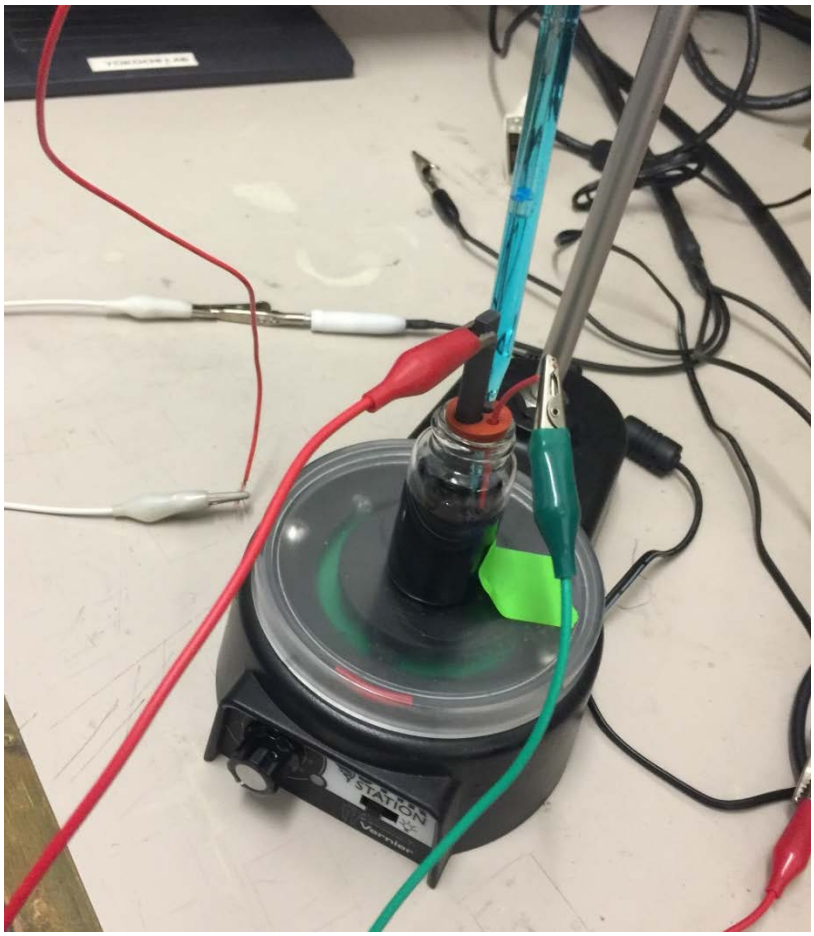

Figure 12: Picture showing the setup of the containment system and the leads from the potentiostat. Green is working, red is counter, and white is reference

The standard reduction potential for the 4/5 reaction is 1.0 V (reaction shown below), and this is driven up by the presence of H^+ ions from the dissociation of the sulfuric acid in the electrolyte; additionally, the standard reduction potential of the $Cu/CuSO_4$ electrode is about 300 mV.

$$VO_2^+ + 2H^+ + e^- \leftrightharpoons VO^{2+} + H_2O$$

An Open Circuit Potential (OCP) was done before every test to ensure that the setup was connected properly, with the expected value being around 750 mV. Each Tafel sweep was done from 250 mV below to 250 mV above the OCP at a sweep rate of 0.167 mV / s and a measurement acquired every 1 s, with the electrolyte being stirred at 85% of the plate's maximum power. The electrolyte was stirred to prevent mass transfer from affecting the system. Each Cyclic Voltammogram had a max voltage of 0.6 V above the OCP and a minimum of 0.5 V below the OCP, with a sweep rate of 10 mV / s and a step size of 2 mV, and the electrolyte was not stirred so that the mass transfer limitations of the system would be observed. Each electrode was put through a total of 2000 cycles of cyclic voltammetry, with the test stopped after cycles 10, 50, 90, 200, 300, 500, 700, 1000, 1500, and 2000 to perform a Tafel sweep.

4. Results and Discussion

4.1. Electrode Working Area

The primary method of analysis of a cyclic voltammogram (CV) is done using the Randles-Sevcik equation, shown in Equation 3. The equation parameters are i_P, the peak current of a cycle in Amps; n, the number of electrons transferred; A, the working electrode surface area in cm^2; D, the diffusion coefficient in cm^2 / s; C, the concentration of the electroactive species in mol / cm^3; and v, the scan rate in V / s.[16]

$$i_P = (2.65 * 10^5)\, n^{2/3}\, A\, D^{1/2}\, C\, v^{1/2} \tag{3}$$

To properly use Equation 3, the diffusion coefficient was estimated using the Wilke-Chang correlation, in the following manner.[19]

$$D_{AB} = (7.4 * 10^{-8}) \frac{(\varphi_B\, M_B)^{1/2}\, T}{{V_A}^{0.6}\, \mu_B} \tag{4}$$

Where the diffusing species, A is vanadyl sulfate, and solvent species B is water,

φ_B = 2.4[19]
M_B = 18 g / mol
T = 298.15 K
V_A = 22 cm^3 / mol[20]
μ_B = 1 cP

$$D_{AB} = 2.27 *\ 10^{-5}\ \frac{cm^2}{s}$$

In analyzing the CVs, the target parameter is the working electrode area since the peak current can be pulled from the raw data produced by the potentiostat. To do this, Equation 3 was rearranged into the following.

$$A = \frac{i_P}{(2.65 * 10^5)\, n^{2/3}\, D^{1/2}\, C\, v^{1/2}} \tag{5}$$

The active area of the working electrode was calculated at each interval specified in Section 3.3 using Equation 5 and the results are shown in Figure 13.

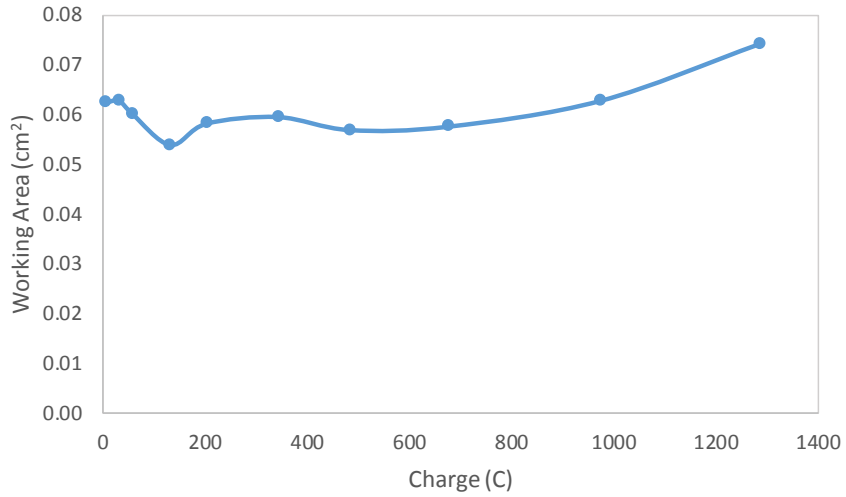

Figure 13: Measured working area of electrode at cycle intervals

Figure 13 shows an interesting pattern in the data. It was expected that the working area would trend downward with increased cycling, but the increase in the active area at the last four intervals shows otherwise. The average working area of the electrode is around 20% of the total area of the working electrode, showing that the wax impregnated took up large portion of the surface area on the face of the electrode. It is possible that this is because as the wax impregnated in the graphite was corroded, more of the graphite was revealed and could act as the active surface for the reaction. Figure 14 shows the CVs of the last 500 cycles of the electrode.

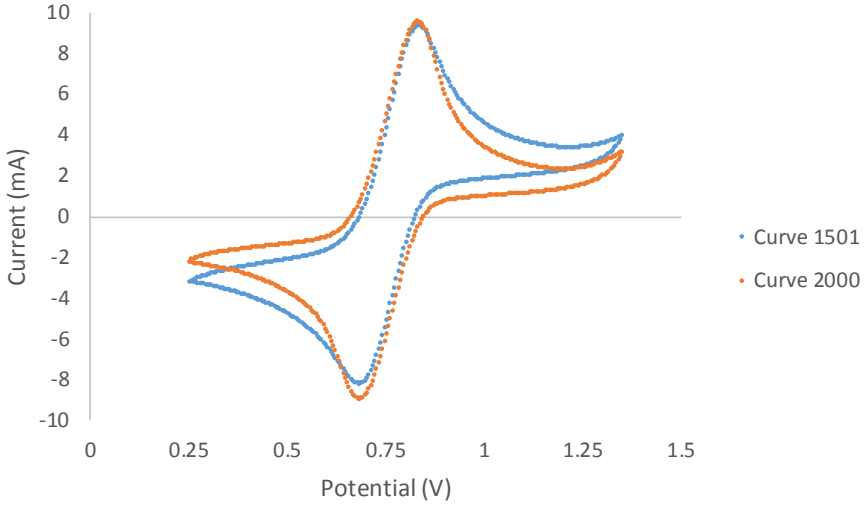

Figure 14: Comparison of the CVs of the final 500 cycles

In Figure 14, it is shown that the peak current does not change much as the electrode is continuing to be cycled, but rather the resultant current after the peak slowly decreases as the electrode is corroded. There is a slight upswing in the current at a high potential, which is the onset of oxygen evolution in the electrode, a major source of degradation within the system. As the electrode degrades, there is little impact on the mass transport within the system, but it is likely that the number of electroactive sites within the electrode decreases. There is also the potential for the concentration of vanadium at the surface to becoming more of an issue at higher cycles. The concentration of each vanadium species affects the solubility of vanadium in the electrolyte, and this coupled with a decrease in active sites on the surface of the electrode would result in a lower current output. It is being assumed that there is no change in the electrolyte throughout the cycling of the electrode and therefore the degradation can be attributed to the electrode. At each interval the OCP was measured, and a small drift was noticed over the 2000 cycles, and this was attributed to a small change in the H^+ concentration, however there was not any other tests (such as ICPMS to look for vanadium precipitate) done to confirm this assumption.

4.2. Exchange Current Density and Transfer Coefficient

Using the equations found in Figure 11, the exchange current density was found from each Tafel plot produced. The linear region was considered between 30 and 60 mV of overpotential for both the anodic and cathodic sweeps. Each line fitted to the points in the linear region had an R^2 value above 0.97. An example of this analysis can be found in the Appendix.

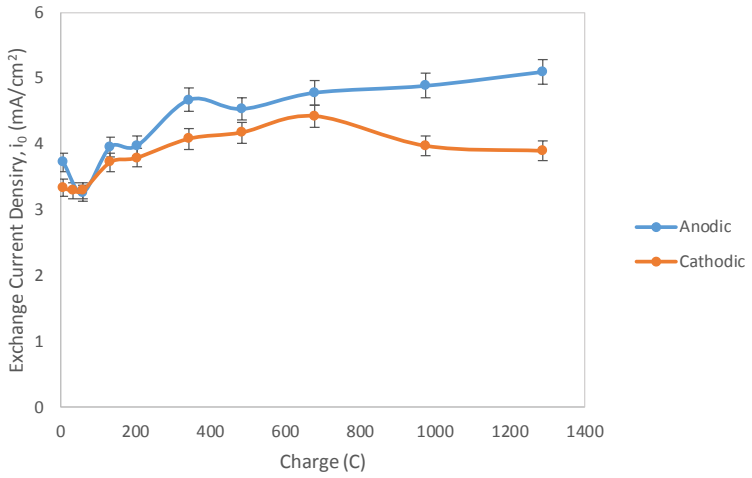

Figure 15: Measured exchange current density as the electrode was aged

Figure 15 shows the change in both the anodic and cathodic exchange current density as working electrode is aged. Ideally, these are the same for both the anode and the cathode, and they are very similar for much of the aging process, then start to separate as the cycles increase. The initial difference is likely to be a result of inherent variation of the electrochemical process and product of the calculations. However, the difference after a high number of cycles is likely due degradation of the electrode and the presence of oxygen-based functional groups on the electrode that influence the kinetics of the redox reaction. Figure 16 shows a trend that perhaps sheds more light on the degradation of the electrode.

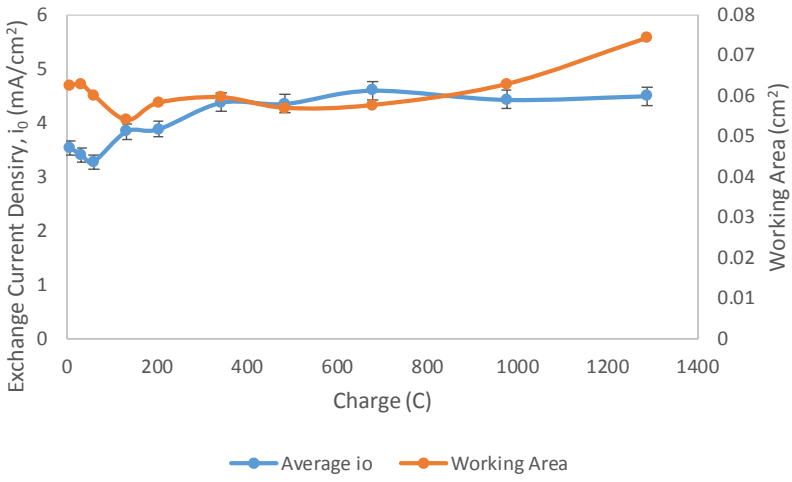

Figure 16: Comparison of the average exchange current density and the working area of the electrode as the electrode was aged

Figure 16 shows that the exchange current density follows a similar trend to the working area of the electrode throughout most of the experiment. The two curves diverge from each other at the end of the cycling, revealing degradation present in the working electrode. While some of the wax was corroded and more of the physical surface area of the electrode being present, number of electrochemical active sites does not follow the same trend as the surface area. This indicates that the density of active sites on the physical surface of the electrode decreases with the aging of the electrode.

A similar analysis was done on the Tafel plots to measure the charge transfer coefficient as the electrode was cycled. These results are shown in Figure 17.

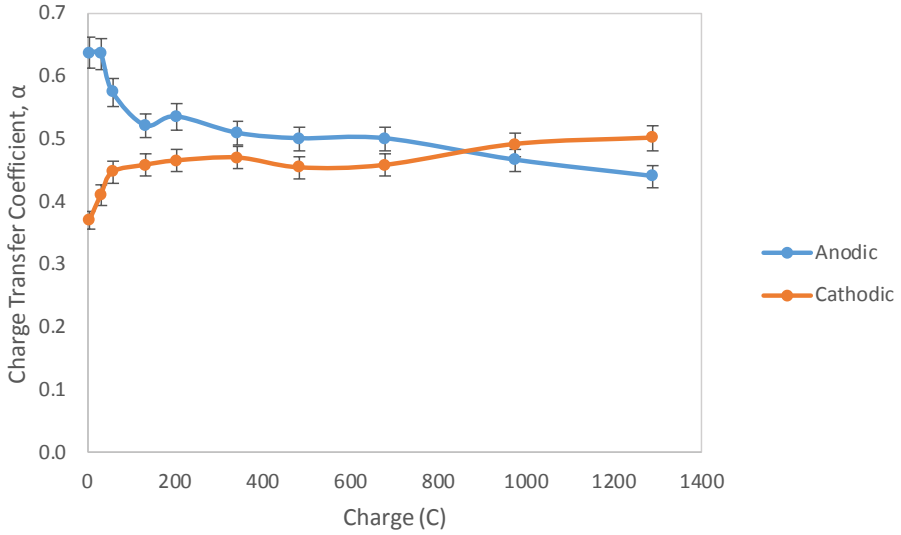

Figure 17: Charge transfer coefficient as the electrode was aged

These results show that there is a significant difference in the anodic and cathodic charge transfer coefficients, especially at low cycle numbers. With the anodic half starting at such a high transfer coefficient, this indicates that, early on, the forward oxidation reaction is favored more than that of the forward reduction reaction. Both transfer coefficients approach and pass 0.5 as the electrode is aged, showing that the degradation of the carbon and increased presence of functional groups greatly changes the kinetics of the redox reaction. This demonstrates that the

4/5 couple is asymmetric and the reversibility of the reaction is dependent upon many different factors within the system.

4.3. Asymmetry of the V(4/5) Redox Couple

Figure 17 shows that there is an asymmetric nature to the vanadium 4/5 redox couple, resulting from kinetics that are not perfectly reversible. Different previous investigations have postulated many different mechanisms that contribute to this, including the carbon surface being oxidized, kinetics of the rate determining step, and there being an intermediate vanadium molecule adsorbed onto the surface. Previous literature has suggested that the breaking of the vanadium-oxygen bond could be considered the rate determining step of the redox reaction.[21] This step would be dependent upon both the oxidized and adsorbed species on the electrode surface, as both species would interact with the vanadium ions differently. Additionally, researchers have postulated the presence of an intermediate step in the reaction resulting in a VO_2^0 molecule that could be adsorbed on the surface or have low solubility in the electrolyte.[21] The many different variables in the system cause this asymmetry and contribute to the early onset of the concentration polarization limitation. The effects of this are demonstrated in Figure 18.

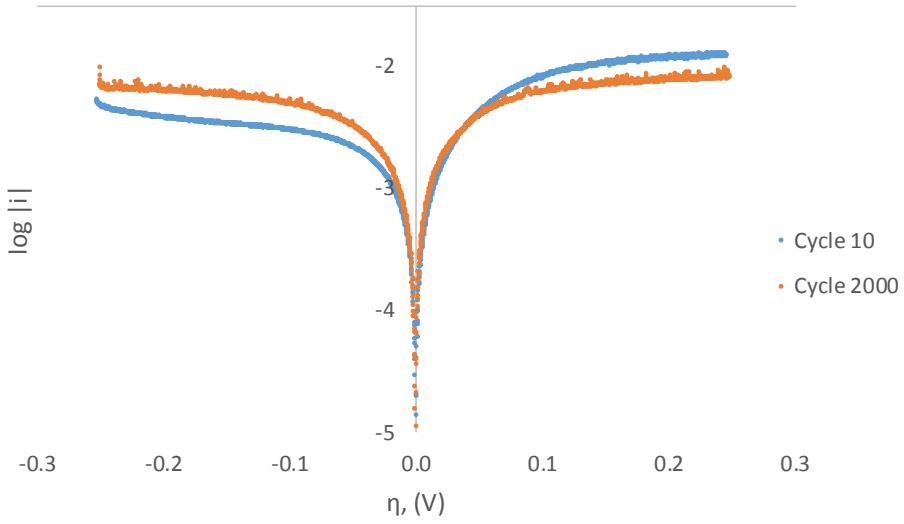

Figure 18: Tafel plots produced after 10 and 2000 cycles of the electrode

This figure shows that there is a significant shift in the Tafel plots produced at the beginning and end of the aging cycles. These results are consistent with what is shown by the change in the charge transfer coefficient in Figure 17, as the later Tafel plots indicate much more reversibility and symmetry than the early plots.

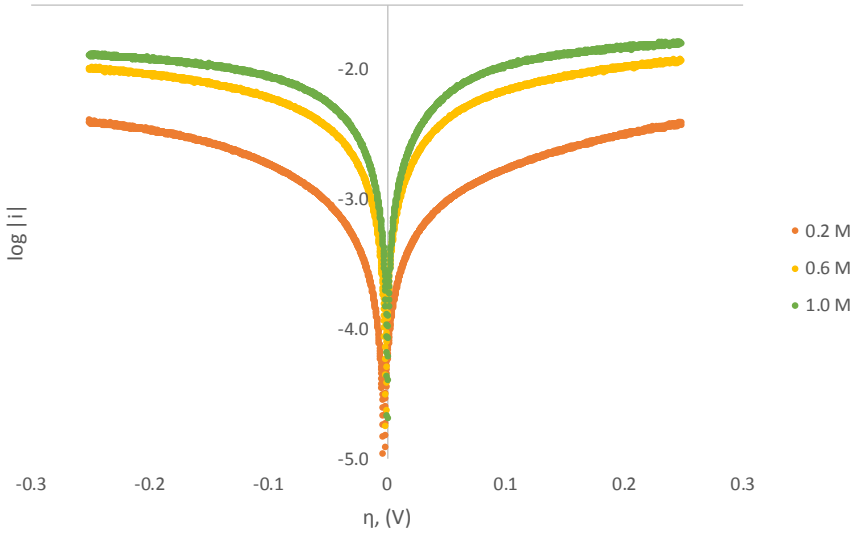

Figure 19: Tafel plots of vanadium concentrations of 0.2, 0.6, and 1.0 M

A short additional experiment was done to investigate the effect of the concentration of vanadium in the electrolyte on the symmetry of the Tafel plot. Figure 19 shows that the balance of the asymmetry shifts as the concentration of vanadium changes. With that meaning at low bulk concentrations, the cathodic current is higher, while at higher bulk concentrations, the anodic current is higher. This provides evidence that there is an intermediate state of vanadium between the redox reactions, and the concentration of this molecule affects the kinetics of the reactions.

5. Conclusions and Future Work

5.1. Conclusions

This thesis conducted an analysis of carbon degradation and kinetics of the 4/5 redox couple of a vanadium sulfate electrolyte. It was shown that the active surface area in the working graphite electrode had increased at the end of 2000 cycles. Cyclic voltammograms also indicated that the mass transport within the electrode is not affected much by cycling, however the steady-state current decreases as a result of less electroactive sites. Through the use of the Tafel equation, the exchange current density was shown to follow a similar trend to the working area of the electrode until large amounts of current had been passed through the electrode, indicating degradation via the presence of oxygen-based functional groups. The Tafel equation was also used to measure the charge transfer coefficient, which showed a distinct asymmetric trend as a result of the many degradation mechanisms affecting the rate determining step. This asymmetric behavior was then shown to have shifted with changing the concentration of the vanadium in the electrolyte.

5.2. Future Work

A more extensive analysis for the data produced could be done using the Butler-Volmer model, as it can individually calculate the exchange current density and charge transfer coefficient for reduction and oxidation. However, that is outside of the scope of this thesis, and would be more ideal under a different electrode setup where one working electrode is always considered the anode, and the other is always considered the cathode. Additionally, this same analysis could be performed on the 2/3 vanadium redox couple. This experiment would prove useful, as the two electrolytes used in a vanadium redox flow battery are V(2/3) and V(4/5).

6. Appendix A

The purpose of this appendix is to show a sample of how the exchange current density and charge transfer coefficient were calculated from a Tafel plot. Figure 17 shows the how the Tafel plot from after 10 cycles was analyzed to produce i_0 and α.

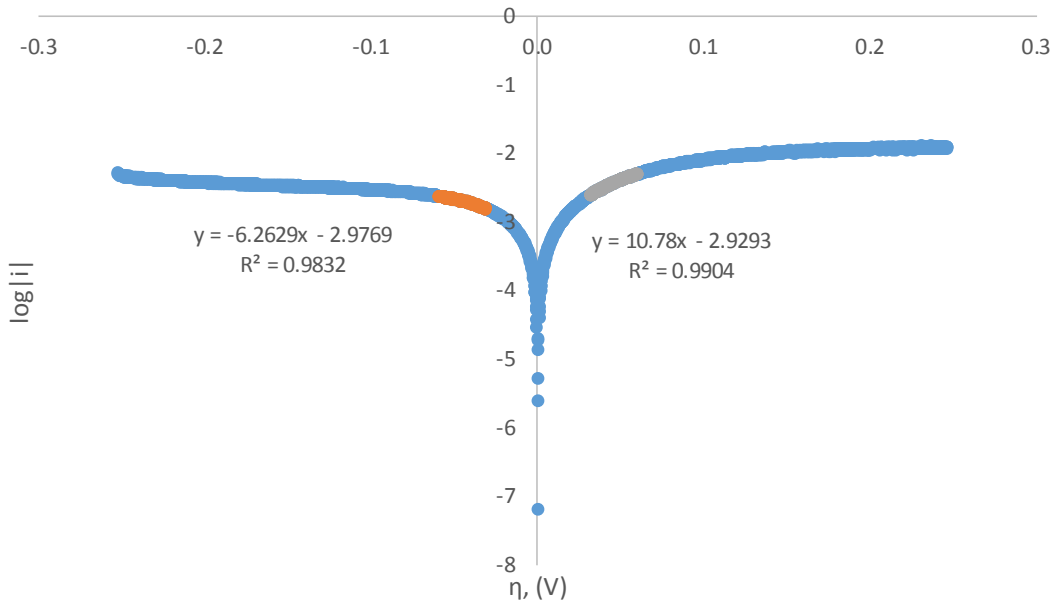

Figure 20: Tafel plot produced after 10 cycles, as analyzed for exchange current density and charge transfer coefficient calculations

These linear equations were confirmed using the LINEST function in Excel, then used to calculate i_0 and α by the following.

$$i_0 = \frac{10^{intercept}}{surface\ area} * 1000$$

For the anodic current,

$$i_0 = \frac{10^{-2.9293}}{0.316} * 1000$$

$$i_0 = 3.72 \frac{mA}{cm^2}$$

$$\alpha = \frac{2.3 * Slope\ R\ T}{F}$$

$$\alpha = \frac{2.3 * 10.78 * 8.314 * 298.15}{96485}$$

$$\alpha = 0.637 \frac{cm^2}{s}$$

For the cathodic current,

$$i_0 = \frac{10^{-2.9769}}{0.316} * 1000$$

$$i_0 = 3.34 \frac{mA}{cm^2}$$

$$\alpha = -\frac{2.3 * Slope\ R\ T}{F}$$

$$\alpha = -\frac{-2.3 * -6.263 * 8.314 * 298.15}{96485}$$

$$\alpha = 0.370 \frac{cm^2}{s}$$

7. References

[1] Brian Kennedy, Two-thirds of Americans give priority to developing alternative energy over fossil fuels. Pew Research Center. [Online] 2017. (Accessed Jan 24, 2017).

[2] Bonneville Power Administration. Operations Info: BPA Balancing Authority Load and Total Wind, Hydro, Fossil/Biomass, and Nuclear Generation, Near-Real-Time. https://transmission.bpa.gov/business/operations/Wind/baltwg.aspx (accessed Mar 11, 2017).

[3] SolarCity. MySolarCity: Powerguide, OSU 35th Street Solar Field Production Data, Jul 16, 2016. https://mysolarcity.com/Share/007c9349-72ba-450c-aa1f-4e5a77b68f79#/monitoring/historical/day?date=2016-07-16 (accessed Mar 11, 2017).

[4] Ian Johnston, Developing world invests more in renewable energy than rich countries for first time, new study says. Independent. [Online] 2017. (Accesssed June 6, 2017).

[5] Denholm, P.; O'Connell, M; Brinkman, G.; Jorgenson, J. *Overgeneration from Solar Energy in California: A Field Guide to the Duck Chart*; TP-6A20-65023; NREL: Golden, CO, 2015.

[6] International Energy Agency *Energy for All, Financing access for the poor*; OECD/IEA: Paris, France, 2011.

[7] Rural Electrification Task Force of EUROBAT's Industrial Battery Committee *Battery Energy Storage for Rural Electrification Systems*; EUROBAT; 2013.

[8] Fong, D. *Sustainable Energy Solutions for Rural Areas and Application for Groundwater Extraction*; GENI; San Diego, CA, 2014.

[9] Chen, S.X.; Gooi, H.B.; Wang, M.Q. Sizing of Energy Storage for Microgrids. *IEEE Transactions on Smart Grid*. **2012**, 3, 142-151.

[10] Kim, J.; Jeon, J.; Kim, S.; Cho, C.; Park, J.H.; Kim, H.; Nam, K Cooperative Control Strategy of Energy Storage System and Microsources for Stabilizing the Microgrid during Islanded Operation. *IEEE Transactions on Power Electronics*. **2010**, 25, 3037-3048.

[11] Denholm, P.; Fernandez, S.J.; Hall, D.G.; Mai, T.; Tegen, S. "Energy Storage Technologies," Chapter 12. National Renewable Energy Laboratory. Renewable Electricity Futures Study, Vol. 2, Golden, CO, 2012.

[12] Dunn, B.; Kamath, H.; Tarascon, J. Electrical Energy Storage for the Grid: A Battery of Choices. *Science*. **2011**, 334, 928-935.

[13] Janse van Rensburg, P.J. Energy Storage in Composite Flywheel Rotors. Masters Dissertation, Stellenbosch University, Stellenbosch, South Africa, 2011.

[14] Maru, H.C.; Dulles, J.F.; Kardas, A.; Paul, L. *Molten Salt Energy Storage Systems*; EY-76-C-02-2888; USDOE; Chicago, Ill; 1978.

[15] Weber, A.Z.; Mench, M.M.: Meyers, J.P.; Ross, P.R.; Gostick, J.T.; Liu, Q. Redox Flow Batteries, a Review. *Journal of Applied Electrochemistry*. **2011**, 41, 1136-63.

[16] Robinson, J.W.; Frame, E.M.S.; Frame, G.M. Undergraduate Instrumental Analysis; 7th edition; Boca Raton, 2014.

[17] Bard, A.J.; Faulkner, L.R.; Electrochemical Methods: Fundamentals and Applications; 2nd edition, John Wiley and Sons, 2007.

[18] Patel, B. University of Brighton. https://i.ytimg.com/vi/1f92vGOridg/maxresdefault.jpg (accessed April 12, 2017).

[19] Welty, J.; Wicks, C.E.; Rorrer, G.L.; Wilson, R.E. Fundamentals of Momentum, Heat and Mass Transfer, 5th edition; John Wiley & Sons: Hoboken, 2007.

[20] Xu, W.; Qin, Y.; Gao, F.; Liu, J.; Yan, C.; Yang, J. Determination of Volume Properties of Aqueous Vanadyl Sulfate at 283.15 to 313.15 K. *Ind. Eng. Chem. Res.* **2014**, 53, 7217-7223.

[21] Gattrell, M.; Qian, J.; Stewart, C.; Graham, P.; MacDougall, B. The electrochemical reduction of VO_2^+ in acidic solution at high overpotentials. *Electrochimica Acta*. **2005**, 51, 395-407